



Electromagnetic field effects on biological materials



Pornthip Keangin^{a,b}, Kambiz Vafai^{b,*}, Phadungsak Rattanadecho^a

^a Department of Mechanical Engineering, Faculty of Engineering, Thammasat University (Rangsit Campus), 99 moo 18, Klong Luang, Pathum Thani 12120, Thailand

^b Department of Mechanical Engineering, Faculty of Engineering, University of California, A363 Bourns Hall, Riverside, CA 2507-0425, USA

ARTICLE INFO

Article history:

Received 24 May 2013

Received in revised form 17 June 2013

Accepted 17 June 2013

Available online 9 July 2013

Keywords:

Biological materials

Electromagnetic field

Finite element

Local thermal non-equilibrium

Porous medium

Temperature profiles

ABSTRACT

In this study, the effect of an imposed electromagnetic field on biological media is analyzed. The local thermal non-equilibrium (LTNE) is taken into account by solving the two-energy equation model for tissue and blood phases. A comprehensive examination of heat transport through biological media is carried out including thermal conduction in tissue and vascular system, blood-tissue convective heat exchange, metabolic heat generation and imposed heat flux. The primary biological media, i.e., bone, liver, cornea, fat, skin and brain are considered in our analysis. The effects of variations of dimensionless electromagnetic wave power and dimensionless electromagnetic wave frequency on the dimensionless tissue and blood temperature profiles are systematically investigated. Results are obtained for a range of dimensionless electromagnetic wave power from 1 to 500 and dimensionless electromagnetic wave frequency from 0.2 to 2. The coupled equations of electromagnetic wave propagation and heat transfer under LTNE assumption are solved using the finite element method (FEM). This investigation provides the essential aspects for a fundamental understanding of heat transport within biological materials while experiencing an applied electromagnetic field such as applications related to the cancer thermal ablation and can be used as a guideline for these types of treatments.

© 2013 Elsevier Ltd. All rights reserved.

1. Introduction

The modeling of heat transport within biological materials is quite important and has been used extensively in medical thermal therapeutic applications for predicting the temperature during these processes. In recent years, utilization of an imposed electromagnetic field in various applications has increased since the electromagnetic wave can penetrate the surface and is converted into thermal energy very rapidly within the material. Various electromagnetic wave applications have been used in many industrial and household applications. For example, for drying, pasteurization, sterilization, heating processes, etc. [1]. Recently, electromagnetic wave has been introduced as a rapid method of delivering high temperatures to destroy the cancer cells during thermal ablation [2,3]. The imposed electromagnetic field interacts with the material and results in a variety of thermal effects. Various effects such as an increase in temperature as result of electromagnetic radiation on materials are gaining widespread attention, particularly in biological materials [4,5]. However, the resulting thermo-physiologic response of the biological materials subject to an electromagnetic field is not well understood due to the complexity of the configurations in biological materials. The severity of

the physiological effect produced by small temperature increases can be expected to worsen in sensitive organs. An increase of approximately 1–5 °C in human body temperature can cause numerous malformations, temporary infertility in males, brain lesions, and blood chemistry changes [6]. In order to gain insight into the phenomena occurring within the biological materials subject to an imposed electromagnetic field, detailed knowledge of the electromagnetic radiation absorption is necessary. A detailed investigation is necessary to demonstrate the effects of electromagnetic radiation absorption in biological materials. Furthermore, numerical simulation under various conditions can be utilized to demonstrate and indentify the fundamental parameters as well as provide guidance for different applications.

Studies of heat transport through biological materials, involves thermal conduction in tissue and vascular system, blood-tissue convection and perfusion (through capillary tubes within the tissues) as well as metabolic heat generation [6–10]. Wessapan et al. [6] have carried out a numerical analysis of specific absorption rate (SAR) and heat transfer in human body due to an electromagnetic field leakage. Keangin et al. [10] carried out the numerical simulation of liver cancer treatment using the micro-wave antenna.

A biological tissue can be represented by a microvascular bed with blood flow through many vessels, through which blood flows and can be regarded as a porous structure [7]. Utilizing porous media theory in modeling heat transfer results in fewer

* Corresponding author.

E-mail addresses: vafai@engr.ucr.edu (K. Vafai), ratphadu@engr.tu.ac.th (P. Rattanadecho).

Nomenclatures

a_{tb}	specific surface area between the blood and the tissue (m^2/m^3)
Bi	Biot number, $Bi = \frac{h_{tb} a_{tb} H^2}{K_{t,eff}}$
c_p	specific heat capacity ($J/kg \text{ } ^\circ C$)
E	electric field (V/m)
f	electromagnetic wave frequency (Hz)
h_{tb}	interfacial heat transfer coefficient between the lumen and the tissue ($W/m^2 \text{ } ^\circ C$)
H	height of the biological material (m)
k_0	free space wave number (m^{-1})
K	thermal conductivity ($W/m \text{ } ^\circ C$)
L	length of the biological material (m)
P	electromagnetic wave power (W)
q_s	heat flux at the surface (W/m^2)
Q	heat source (W/m^3)
T	temperature ($^\circ C$)
u	lumen velocity (m/s)
x	longitudinal coordinate (m)
y	transverse coordinate (m)

Greek Symbols

ϵ	porosity (the ratio of the volume fraction of the vascular space to the space occupied by the extra-vascular space) (-)
η	dimensionless transverse coordinate, $\eta = \frac{y}{D}$

Φ	dimensionless heat generation within the biological material, $\Phi = \frac{(1-\epsilon)HQ_{met}}{q_s}$
κ	ratio of the effective blood thermal conductivity to that of the tissue, $\kappa = \frac{K_{b,eff}}{K_{t,eff}}$
ρ	density (kg/m^3)
θ	dimensionless temperature, $\theta = \frac{K_{t,eff}((T)-T_s)}{q_s H}$
μ	magnetic permeability (H/m)
γ	permittivity (F/m)
σ	electric conductivity (S/m)
ω	angular frequency (rad/s)

Subscripts

b	blood phase
c	cut off
eff	effective property
ext	external
met	metabolic
r	relative
s	surface
t	tissue phase
tb	tissue to blood
0	free space, initial condition

Abbreviations

FEM	finite element method
LTNE	local thermal non-equilibrium

assumptions as compared to different established bioheat transfer models [7–9]. Depiction of heat transport through a porous medium has been of interest for many decades. Two different models are used for analyzing heat transfer in a porous medium; local thermal equilibrium (LTE) and local thermal non-equilibrium (LTNE) [11–15]. The LTE model is based on the assumption that the tissue phase temperature is equal to blood phase temperature everywhere in the porous medium and referred to as the one equation model [7,11–13]. This assumption is not suitable for a number of physical situations [7]. In recent years, the LTNE model has received more attention to demonstrate the heat transport in biolog-

ical media [7–9,16,17]. Utilizing the porous media theory, LTNE between the tissue and the blood phase is addressed and the tissue-blood convective heat exchange is taken into account. Volume averaging over each of the tissue and blood phases results in energy equations for each individual phase. Studies of heat transport under LTNE in biological media has been established in the literature [8,9]. Mahjoob and Vafai [8] analyzed characterization of heat transport through biological media incorporating hyperthermia treatment, utilizing the LTNE model. They had obtained detailed exact solutions for the tissue and blood temperature profiles. Mahjoob and Vafai [9] analyzed characterization of bioheat transport

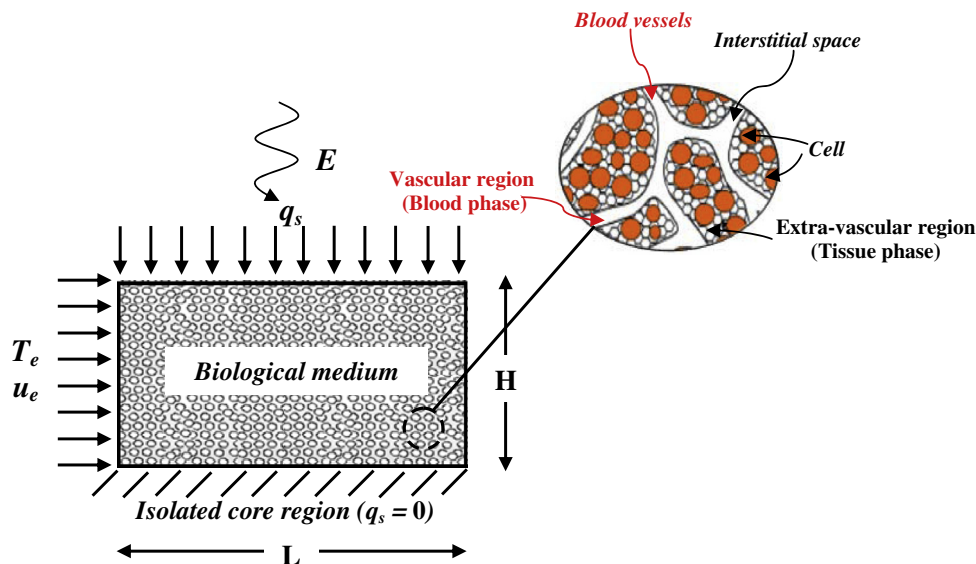


Fig. 1. Schematic diagram of a biological medium subject to an electromagnetic field.

Table 1
Thermal and dielectric properties of biological media used in the computations [6,24–30].

Biological materials	Density ρ (kg/m ³)	Thermal conductivity K (W/m °C)	Specific heat capacity C_p (J/kg °C)	Porosity ϵ	Relative permittivity γ_r	Electric conductivity σ (S/m)
Liver	1030 [6]	0.497 [6]	3600[6]	0.6 [24]	43.0 [6]	1.69 [6]
Brain	1038 [30]	0.535 [30]	3650 [30]	0.2 [26]	45.805 [30]	0.765 [30]
Cornea	1050 [29]	0.58 [29]	4178 [29]	0.6 [29]	52.0 [29]	1.85 [29]
Skin	1125 [6]	0.35 [6]	3437 [6]	0.2 [27]	44.86 [6]	0.92 [6]
Bone	1038 [6]	0.436 [6]	1300 [6]	0.75 [28]	44.80 [6]	2.10 [6]
Fat	916 [6]	0.22 [6]	2300 [6]	0.17 [25]	5.97 [6]	0.09 [6]
Blood	1058 [6]	0.45 [6]	3960 [6]	1.0 [27]	58.30 [6]	2.54 [6]

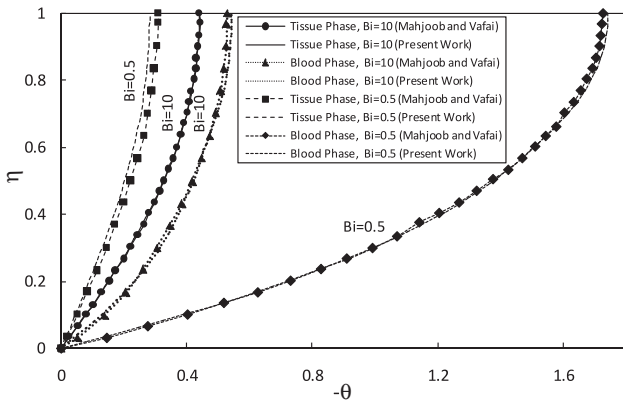


Fig. 2. Comparison of the tissue and blood temperature profiles obtained from the present numerical results and the analytical results by Mahjoob and Vafai [8] for $\epsilon = 0.1$, $\Phi = 0$ and $\kappa = 0.111$ at $Bi = 10$ and $Bi = 0.5$.

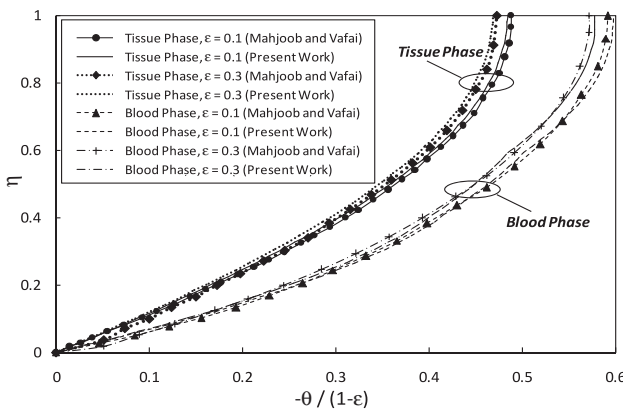
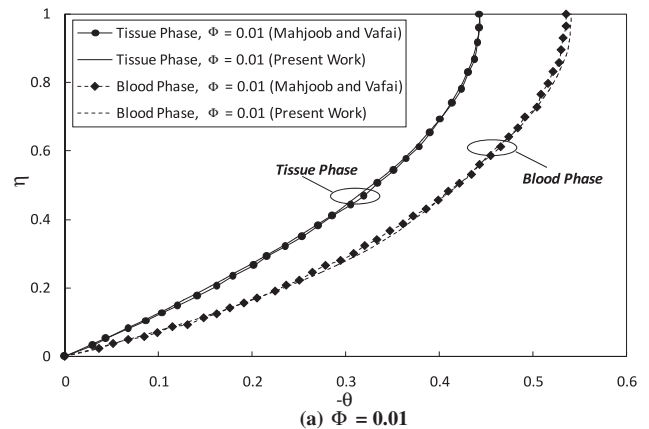


Fig. 3. Comparison of the tissue and blood temperature profiles obtained from the present numerical results and the analytical results by Mahjoob and Vafai [8] for $\Phi(1 - \epsilon) = 0.022$ and $\kappa = 0.111$ at $Bi = 10$ with $\epsilon = 0.1$ and $\epsilon = 0.3$.

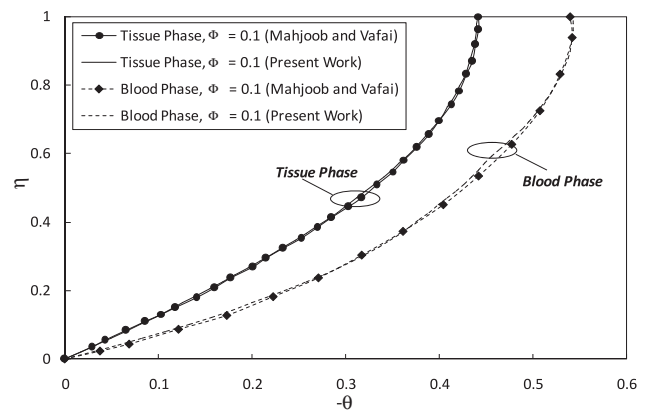
through a dual layer biological media. The effect of the vascular volume fraction and metabolic heat generation on the temperature within the biological media was discussed in their work and detailed exact solutions were obtained. Belmiloudi [18] analyzed the temperature distribution in biofluid heat transfer during thermal therapy based on LTNE model. Afrin et al. [19] presented a model of thermal lagging in living biological tissue based on LTNE heat transfer model between tissue, arterial and venous bloods. It was found that the phase lag times for heat flux and temperature gradient are identical for the case when the tissue and blood have the same properties.

While there have been studies on heat transport based on LTNE assumption, very few works have studied electromagnetic wave propagation coupled with heat transfer based on LTNE model.

Furthermore, only few prior studies have concentrated on the effect of electromagnetic field such as electromagnetic wave power and electromagnetic wave frequency particularly as applied to biological materials due to the complexity of the problem. To gain insight into the process occurring within the biological tissues subject to an imposed electromagnetic field, it is essential to study temperature distribution within a biological tissue during cancer thermal ablation. As such it is necessary to obtain a detailed knowledge of the electromagnetic radiation absorption coupled with heat transport. Biological tissues have different properties and response times for disturbances, especially when subject to an electromagnetic field. In order to understand the thermal response of the biological tissues subject to an electromagnetic field, knowledge of the thermal response in various biological tissues is required.



(a) $\Phi = 0.01$



(b) $\Phi = 0.1$

Fig. 4. Comparison of the tissue and blood temperature profiles obtained from the present numerical results and the analytical results by Mahjoob and Vafai [8] for $\epsilon = 0.1$ and $\kappa = 0.111$ at $Bi = 10$ where (a) $\Phi = 0.01$ and (b) $\Phi = 0.1$.

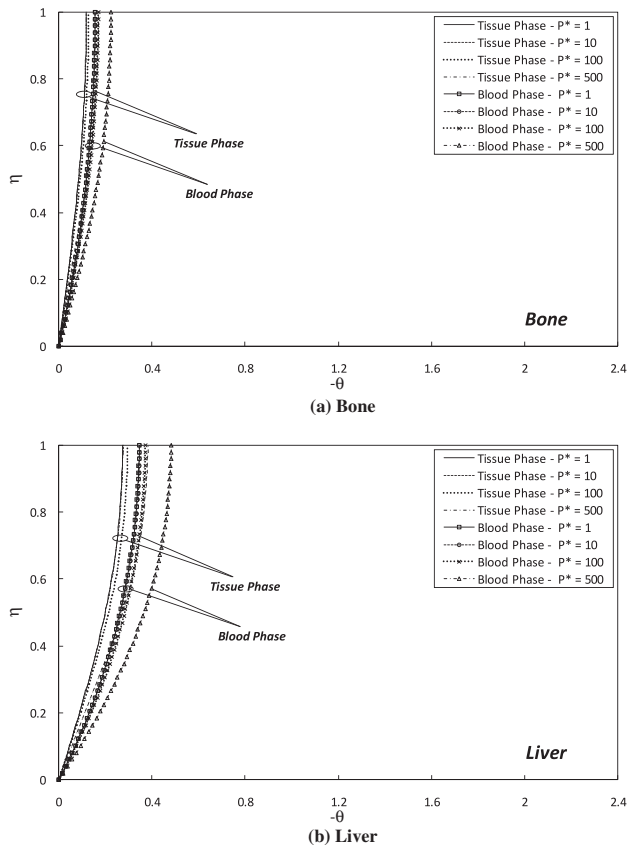


Fig. 5. Effects of the electromagnetic wave power on the tissue and blood temperature profiles in different biological media for $\Phi = 0.1$ and $f^* = 0.6$ at $Bi = 10$ for (a) Bone and (b) Liver.

Modeling of heat transport coupled with electromagnetic wave propagation in biological media is required to investigate the cited applications. The aim of this study is to analyze and demonstrate the effect of electromagnetic field, namely the electromagnetic wave power (P^*) and electromagnetic wave frequency (f^*) on the tissue and blood temperature profiles in biological media. The heat flux intensity effects on biological media are investigated and characterized to establish the thermal signature in biomedical applications such as thermal ablation. This study focuses attention on primary biological materials in the human body such as bone, liver, cornea, fat, skin and brain. The dimensionless tissue and blood temperature profiles in various biological materials, obtained by numerical solution of heat transfer coupled with electromagnetic wave propagation under LTNE assumption, are presented. The effects of variations of electromagnetic wave power (P^*) from 1 to 500 and electromagnetic wave frequency (f^*) from 0.2 to 2 on tissue and blood temperature profiles are systematically investigated. (P^*) is chosen in the range of 1–500 for simulations in this study as it corresponds to the input electromagnetic power for destroying cancer cells through a thermal ablation process. In addition, (f^*) is chosen in the range of 0.2–2 for simulations as this frequency range corresponds to the electromagnetic band which is used most frequently in applications related to studies on the effects of electromagnetic field on biological materials. The presented results provide the essential aspects for a fundamental understanding of the effects of an imposed electromagnetic field on biological materials under LTNE. Furthermore, the electromagnetic field effect on heat transport patterns in biological tissues is systematically investigated. The results from this study can be used as a guideline for biomedical applications such as cancer thermal ablation for various biological tissues [30].

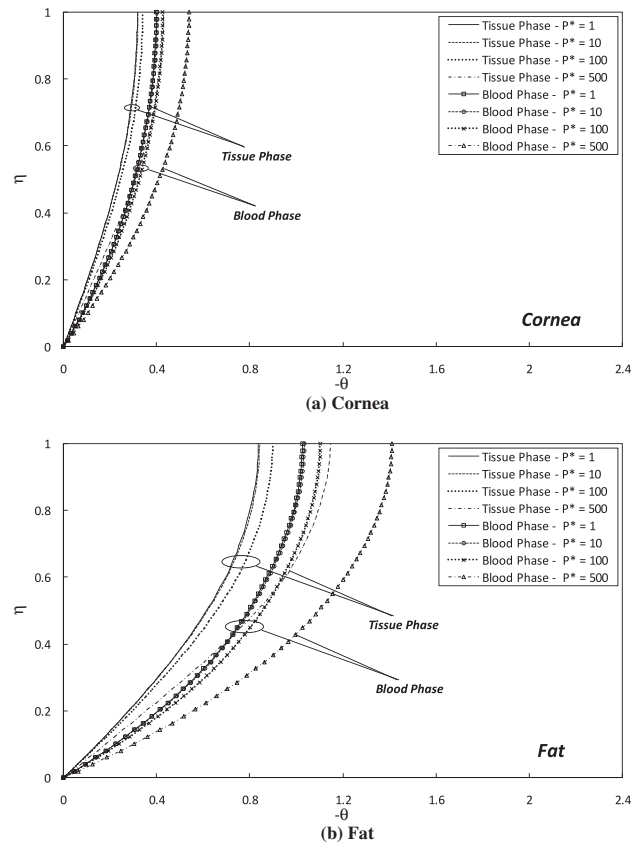


Fig. 6. Effects of the electromagnetic wave power on the tissue and blood temperature profiles in different biological media for $\Phi = 0.1$ and $f^* = 0.6$ at $Bi = 10$ for (a) Cornea and (b) Fat.

2. Problem description

Biological media generally consist of three components i.e. blood vessels, cells and interstitial space [8,20]. Further, biological media can be categorized as vascular region (blood vessels) and extra-vascular region (cells and the interstitial space). The whole anatomical structure can be represented as a blood saturated tissue represented by a porous medium [8], through which the blood infiltrates. The vascular region is regarded as a blood phase and extra-vascular region is regarded as a tissue (solid matrix) phase, as illustrated in Fig. 1.

A two-dimensional model is considered in this work since the biological media is considered homogenous, isotropic and saturated with blood. This model can minimize the computational time while maintaining good resolution and efficiency. In order to investigate the electromagnetic field effects on different biological media, a rectangular slab where H and L denote the height and length of each biological media is considered. The biological medium is subjected to a uniform electromagnetic flux from the top. The electromagnetic external heat source and heat flux represent the imposed energy which is utilized to destroy cancer cells for combined heating during a thermal ablation process. Heat flux represents the heating of a surface while the external heat source represents the electromagnetic energy source such as microwave energy. Electromagnetic irradiation can penetrate the material surface and is converted into thermal energy within the material. This results in a very rapid temperature increase throughout the material that may lead to decomposition of cancer cells. This is a combined heating which can develop into an efficient heating for destroying the cancer cells during the thermal ablation process. The biological media is considered homogenous, isotropic and saturated with

blood. Blood flow is assumed to be hydraulically and thermally fully developed [8]. Natural convection is assumed to be negligible. There is no phase change or chemical reaction within the biological media. The tissue and blood local heat exchange, while the biological medium is subjected to an electromagnetic field, is addressed and the tissue and blood temperature profiles are established in this study.

3. Analysis

Analysis of electromagnetic wave propagation and heat transfer in biological media induced by an electromagnetic field is presented here. The system of governing equations as well as initial and boundary conditions are solved numerically using the finite element method (FEM).

3.1. Electromagnetic wave propagation analysis

The electromagnetic wave propagation in the biological media is modeled on a two-dimensional basis and is calculated using Maxwell's equations, which describe the interdependence of the electromagnetic field. The general form of Maxwell's equations for transverse electric wave (TE) mode is derived assuming a harmonic propagation and is simplified to demonstrate the electromagnetic field in a biological medium [6]:

$$\nabla \times \left(\frac{1}{\mu_r} \nabla \times \vec{E}_z \right) - \left(\gamma_r - \frac{j\sigma}{\omega\gamma_0} \right) k_0^2 \vec{E}_z = 0 \quad (1)$$

where \vec{E}_z is the electric field intensity in the z-direction (V/m), μ_r the relative permeability, γ_r the relative permittivity, $\gamma_0 = 8.8542 \times$

10^{-12} F/m the permittivity of free space, σ the electric conductivity (S/m), $\omega = 2\pi f$ the angular frequency (rad/s) and k_0 is the free space wave number (m^{-1}) and $j = \sqrt{-1}$.

3.1.1. Boundary conditions for the electromagnetic wave propagation analysis

When an electromagnetic field propagates in a biological medium, it is absorbed by the medium and converted into internal heat generation, which causes its temperature to rise. Therefore, boundary conditions for analyzing electromagnetic wave propagation, as shown in Fig. 1, are considered as follows.

The biological medium is subjected to a uniform wave flux from the top. Therefore, at the top boundary of the considered domain, an electromagnetic simulator employs TE wave propagation port with a specified electromagnetic field power:

$$S = \int (\vec{E} - \vec{E}_1) \cdot \vec{E}_1 / \int \vec{E}_1 \cdot \vec{E}_1 \quad (2)$$

The outer sides of the biological media are considered as an electric conductor boundary condition. Therefore, electric field intensity in the z-direction vanishes at these sides.

$$\vec{E}_z = 0 \quad (3)$$

3.2. Heat transfer analysis

The anatomical structure is modeled as a biological medium consisting of tissue and blood phases. The steady state volume-averaged governing equations describing the heat transfer phenomenon for tissue and blood phases incorporating metabolic heat generation and an imposed electromagnetic field under LTNE conditions can be represented as [8]:

Tissue phase:

$$K_{t,eff} \nabla_y^2 \langle T_t \rangle^t - h_{tb} a_{tb} \langle \langle T_t \rangle^t - \langle T_b \rangle^b \rangle + (1 - \varepsilon) Q_{met} + (1 - \varepsilon) Q_{t,ext} = 0 \quad (4)$$

Blood phase:

$$K_{b,eff} \nabla_y^2 \langle T_b \rangle^b + h_{tb} a_{tb} \langle \langle T_t \rangle^t - \langle T_b \rangle^b \rangle + \varepsilon Q_{b,ext} = \varepsilon \rho c_p \langle u \rangle^b \frac{\partial \langle T_b \rangle^b}{\partial x} \quad (5)$$

where,

$$K_{b,eff} = \varepsilon K_b \quad (6)$$

$$K_{t,eff} = (1 - \varepsilon) K_t \quad (7)$$

where subscripts *eff*, *t* and *b* represent the effective value, tissue and blood phase, respectively, *T* the temperature ($^{\circ}C$), ρ the density (kg/m^3), c_p the specific heat capacity ($J/kg^{\circ}C$), K the thermal conductivity ($W/m^{\circ}C$), ε the porosity which is the ratio of the volume fraction of the vascular space, u the blood phase average velocity (m/s), h_{tb} the blood to tissue interfacial heat transfer coefficient ($W/m^2^{\circ}C$) and a_{tb} is the specific surface area between the blood and the tissue (m^2/m^3).

In Eq. (4), the first, second, third and fourth on the left-hand side of equation denote heat conduction, interstitial convection heat transfer, metabolic heat generation and external heat source (heat generation by the electromagnetic field) term, respectively. The bulk blood flow term appears on the right-hand side of the blood phase energy equation (Eq. (5)). It can be seen in Eqs. (4) and (5) that the tissue and blood phases are coupled via the interstitial convective heat transfer term. The interstitial term accounts for the convective heat transfer between the blood and the peripheral tissues. Furthermore, Eqs. (4) and (5) are coupled to the electromagnetic wave propagation equation (Eq. (1)) through Eq. (8).

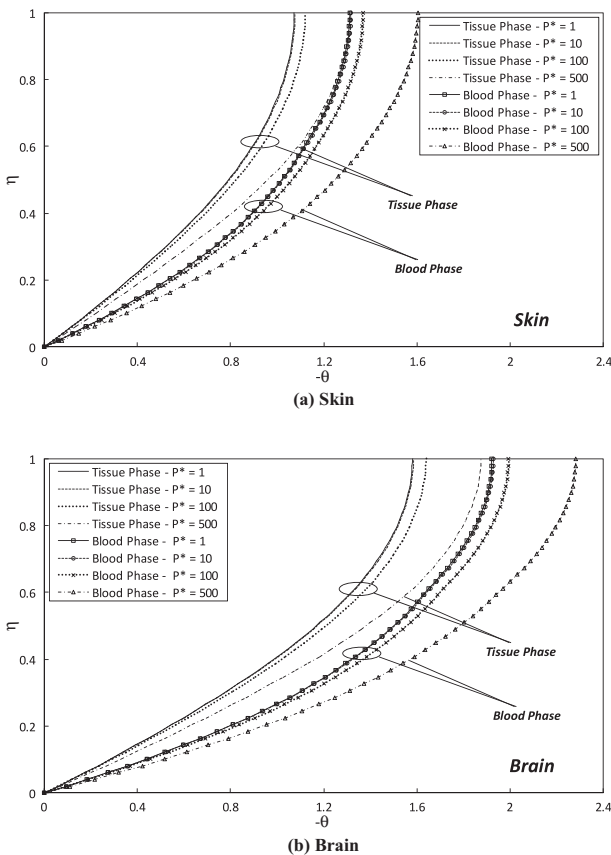


Fig. 7. Effects of the electromagnetic wave power on the tissue and blood temperature profiles in different biological media for $\Phi = 0.1$ and $f^* = 0.6$ at $Bi = 10$ for (a) Skin and (b) Brain.

The computational scheme starts with computing an external heat source term by running an electromagnetic wave propagation calculation and subsequently solving the tissue and blood temperatures in Eqs. (4) and (5) in biological materials. The proposed model is reasonable and adequate for effectively analyzing the essential aspects for a fundamental understanding of heat transport within biological materials subject to an electromagnetic field.

It should be noted that Q_{met} is the metabolic heat generation (W/m^3) while the external heat source is represented by Q_{ext} . The Q_{ext} is equal to the resistive heat generated by electromagnetic field and can be defined as [21]:

$$Q_{ext} = \frac{\sigma |\vec{E}_z|^2}{2} \tag{8}$$

Our external heat source is evaluated in Eq. (8), which is calculated through the electromagnetic wave propagation analysis.

3.2.1. Boundary conditions for the heat transfer analysis

As seen in Fig. 1, the biological medium is subjected to an electromagnetic flux from the top. The imposed heat flux can be represented under the LTNE conditions, based on the work of Mahjoob and Vafai [8], Lee and Vafai [11] and Marafie and Vafai [13] as follows:

$$q_s = -K_{b,eff} \frac{\partial \langle T_b \rangle^b}{\partial y} \Big|_{y=H} - K_{t,eff} \frac{\partial \langle T_t \rangle^t}{\partial y} \Big|_{y=H} \tag{9}$$

The temperature at the interface of the biological media's surface is likely to be uniform regardless of whether it contacts the tissue solid matrix or the blood. As such the temperature of the tissue and the blood at the biological media's surface will be the same [8,11,13,22,23]:

$$\langle T_b \rangle^b \Big|_{y=H} \approx \langle T_t \rangle^t \Big|_{y=H} \approx T_s \tag{10}$$

The core region of the biological medium ($y = 0$) is away from the heat transfer interaction used and is considered to act as an insulated boundary as shown in Fig. 1:

$$q_s = 0 \tag{11}$$

The initial temperature of the biological medium is assumed to be uniform and at the normal body temperature:

$$T(t_0) = 37^\circ C \tag{12}$$

3.3. Non dimensionalization

The numerical results are presented in a dimensionless form. The non-dimensional temperature profiles are plotted against a dimensionless vertical scale, η . These dimensionless variables are defined as:

$$\eta = \frac{y}{D}, \quad \kappa = \frac{K_{b,eff}}{K_{t,eff}}, \quad Bi = \frac{h_{tb} a_{tb} H^2}{K_{t,eff}},$$

$$\theta = \frac{K_{t,eff} \langle \langle T \rangle \rangle - T_s}{q_s H}, \quad \Phi = \frac{(1 - \epsilon) H Q_{met}}{q_s} \tag{13}$$

The dimensionless electromagnetic wave power and dimensionless electromagnetic wave frequency are defined as:

$$P^* = \frac{P}{q_s H^2}, \quad f^* = \frac{f}{f_c} \tag{14}$$

where f_c is the cut off frequency (lowest propagation frequency) of the microwave in TE mode.

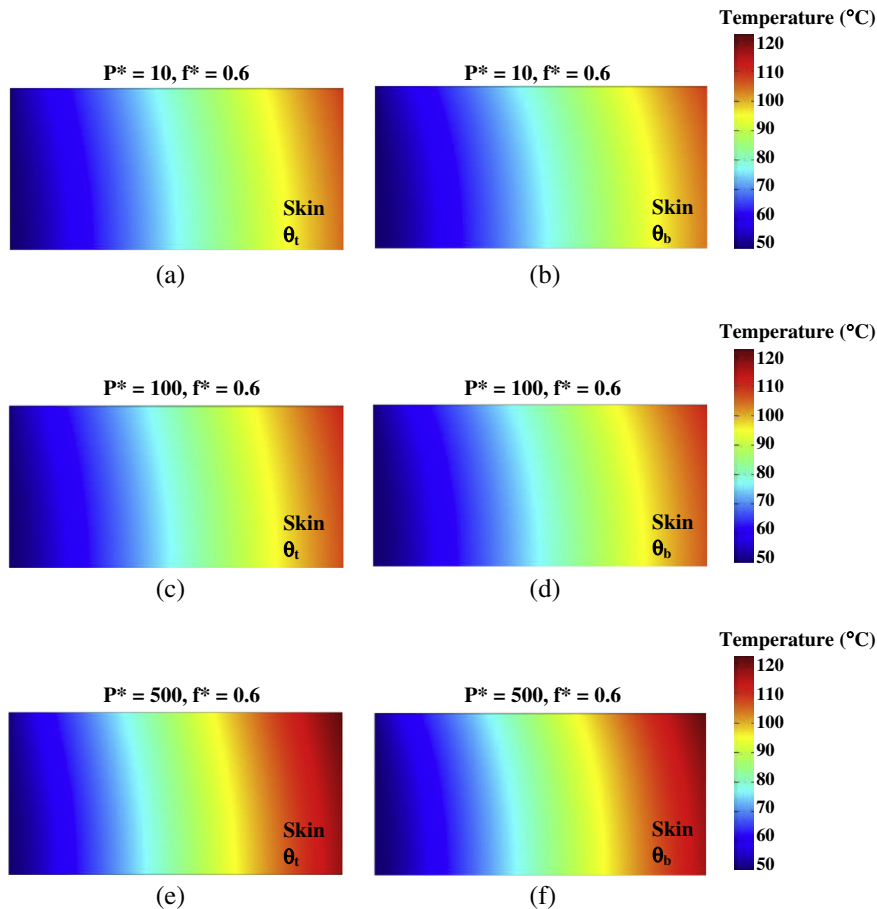


Fig. 8. Effect of the electromagnetic wave power variation on the tissue and blood temperature contours of skin for $\Phi = 0.1$ and $f^* = 0.6$ at $Bi = 10$.

4. Numerical simulations

The heat transport in a biological medium is expressed through Eqs. (4)–(7). These equations are coupled to Maxwell’s equations through Eq. (8). Eqs. (1)–(12) are solved numerically using a FEM via COMSOL™ Multiphysics to demonstrate the phenomenon that occurs in the biological media exposed to an electromagnetic field. The two-dimensional model is discretized using triangular elements, and the Lagrange quadratic is used to approximate temperature profile variations across each element. The biological media comprises six types of tissue including bone, liver, cornea, fat, skin and brain. These biological media have different thermal and dielectric properties and porosities. We assume that the thermal and dielectric properties and porosity of each biological medium are constant. The thermal and dielectric properties and porosities of biological media used in the computations are listed in Table 1 [6,24–30]. Each biological medium is assumed to be homogeneous and electrically as well as thermally isotropic.

5. Results and discussion

5.1. Validation

In order to verify the accuracy of the present model, the numerical results for the case without an electromagnetic field are validated against the analytical results with the same conditions obtained by Mahjoob and Vafai [8]. In the works of Mahjoob and Vafai [8] analytical solutions for heat transport through biological

media incorporating hyperthermia treatment and subject to an imposed heat flux are established. The comparison of dimensionless tissue and blood temperature profiles with the analytical results obtained by Mahjoob and Vafai [8] at $Bi = 10$ and $Bi = 0.5$ are displayed in Fig. 2. The following parameters are used to generate the results: $\varepsilon = 0.1$, $\Phi = 0$ and $\kappa = 0.111$. It can be seen that the dimensionless tissue and blood temperature profiles are in excellent agreement with the analytical results obtained by Mahjoob and Vafai [8]. Fig. 2 also indicates that a decrease in the internal heat exchange ($Bi = 0.5$) results in a larger tissue and blood temperature difference while displaying the importance of utilizing the LTNE model.

Fig. 3 illustrates the comparison of dimensionless tissue and blood temperature profiles with the analytical results obtained by Mahjoob and Vafai [8] at different porosities. The tissue and blood temperature profiles for $\Phi(1 - \varepsilon) = 0.022$ at $Bi = 10$ where $\varepsilon = 0.1$ and 0.3 are shown in Fig. 3. A very good agreement is observed for all of the cited comparisons. This figure also shows that a decrease in the porosity results in a larger deviation between the tissue temperature and that of the blood.

Based on the cited values in Mahjoob and Vafai [8], a representative metabolic heat generation is utilized for some of the comparisons. The comparison of dimensionless tissue and blood temperature profiles with the analytical results obtained by Mahjoob and Vafai [8] with variations in the metabolic heat generation for $\varepsilon = 0.1$ at $Bi = 10$ are displayed in Fig. 4. Fig. 4(a) and 4(b) show the tissue and blood temperature profiles for $\Phi = 0.01$ and 0.1 , respectively. Comparing the results for both metabolic heat generation values indicates a very good agreement as seen in Fig. 4. As

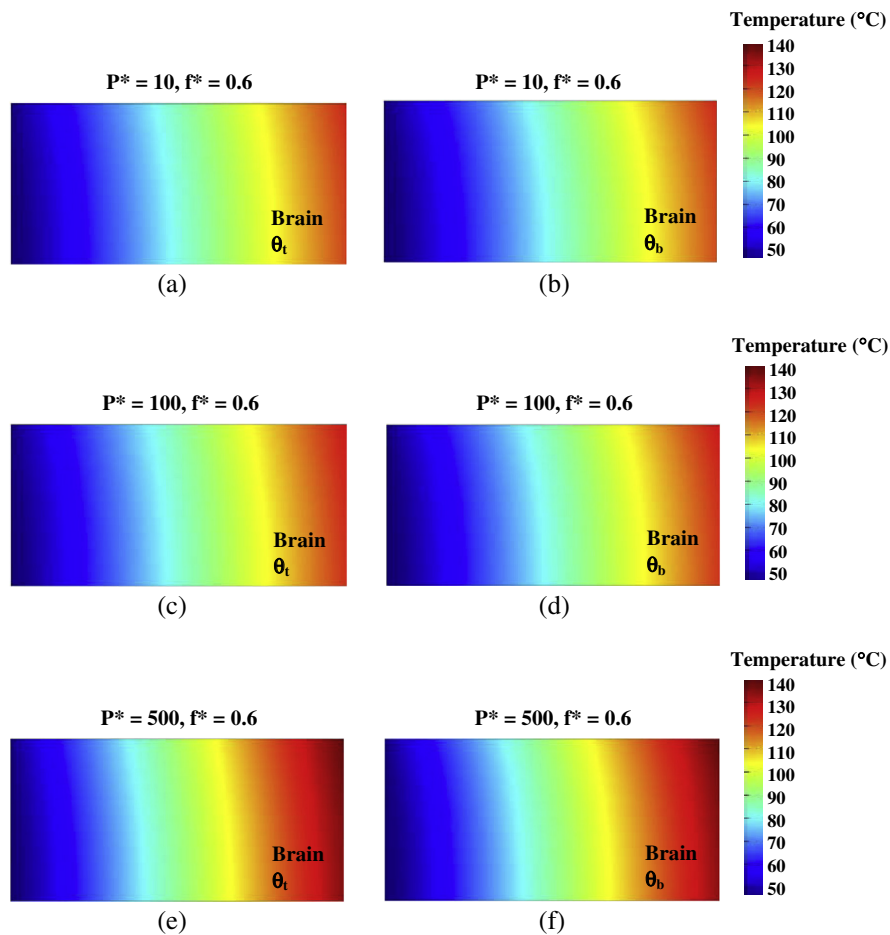


Fig. 9. Effect of the electromagnetic wave power variation on the tissue and blood temperature contours of brain for $\Phi = 0.1$ and $f^* = 0.6$ at $Bi = 10$.

can be seen an increase in the metabolic heat generation enhances the temperature difference between the two phases. Overall, our results in the present study are in excellent agreement with the analytical results by Mahjoob and Vafai [8]. This highly favorable comparison lends confidence in the accuracy of the present numerical model.

5.2. Dimensionless electromagnetic wave power effects

The effects of electromagnetic wave power on the tissue and blood temperature profiles for different types of biological materials are established. In applications for cancer thermal ablation a detailed description of electromagnetic wave power effects is required to address the effectiveness of thermal ablation technique during the process. The effects of dimensionless electromagnetic wave power on the dimensionless tissue and blood temperature profiles for a variety of different biological media exposed to an electromagnetic field are presented in Figs. 5–7. The physical data utilized in these figures are: $\Phi = 0.1$ and $f^* = 0.6$ at $Bi = 10$. The electromagnetic wave power varies from 1 to 500. The dimensionless tissue and blood temperature profiles for bone, liver, cornea, fat, skin and brain are depicted in Figs. 5 (a) and (b), 6(a) and (b) and 7(a) and (b), respectively. It is established that the temperature profile patterns are quite similar for all biological media and the temperature profile of the tissue phase is similar to that of the blood phase. It can be seen in these figures that the electromagnetic wave power significantly influences the rate of temperature increase. As expected, the temperature of the tissue and blood increase with an increase in the electromagnetic wave power for all the considered biological media. This is because an increase in the electromagnetic wave power results in a higher heat generation rate in a biological medium. It can be observed that the dimensionless blood temperature values are higher than the tissue tempera-

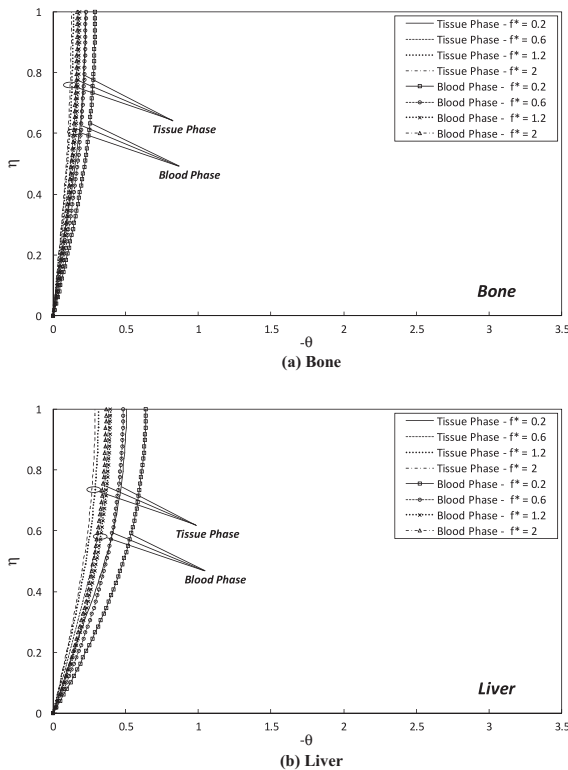


Fig. 10. Effects of the electromagnetic wave frequency on the tissue and blood temperature profiles for $\Phi = 0.1$ and $P^* = 500$ at $Bi = 10$ for biological media for (a) Bone and (b) Liver.

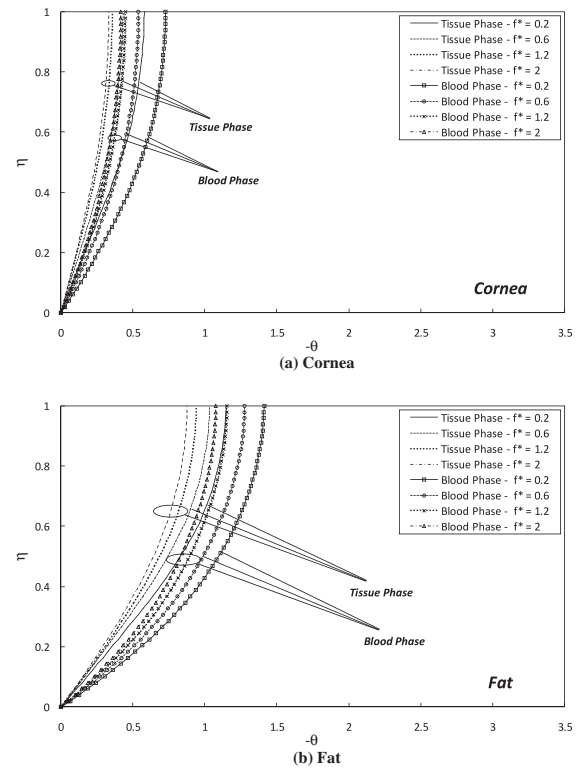


Fig. 11. Effects of the electromagnetic wave frequency on the tissue and blood temperature profiles for $\Phi = 0.1$ and $P^* = 500$ at $Bi = 10$ for biological media for (a) Cornea and (b) Fat.

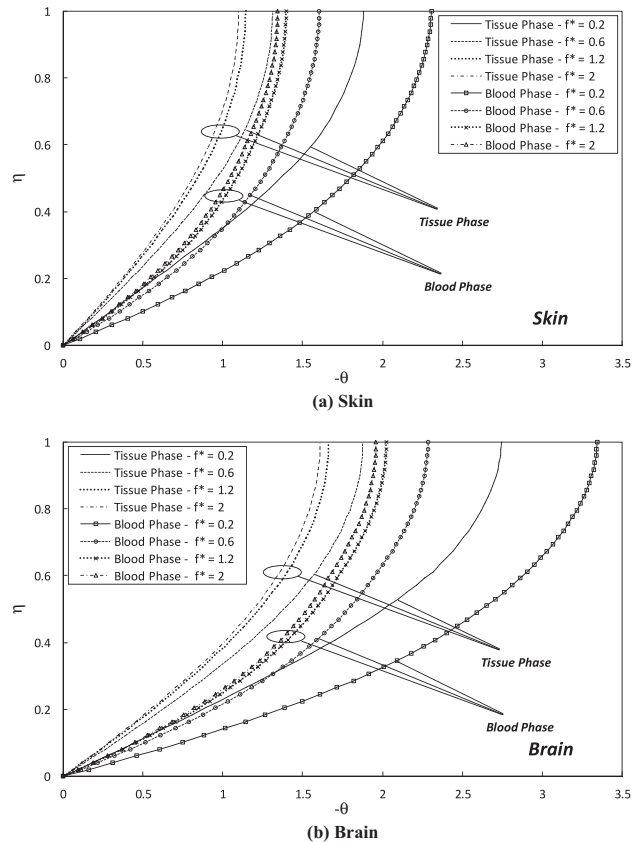


Fig. 12. Effects of the electromagnetic wave frequency on the tissue and blood temperature profiles for $\Phi = 0.1$ and $P^* = 500$ at $Bi = 10$ for biological media for (a) Skin and (b) Brain.

ture for all of the considered biological media at the same electromagnetic wave power due to the different electromagnetic power absorption of tissue and blood temperatures when subjected to an electromagnetic field. Furthermore, the results in these figures also show that an increase in the electromagnetic wave power results in a larger deviation between the tissue temperature and that of the blood. This shows that the error in utilizing an LTE model for heat transfer investigations increases as the electromagnetic wave power increases when an electromagnetic field is imposed.

Comparing the tissue and blood temperature values in each of the biological materials, it can be seen that the brain has the highest tissue and blood temperature values compared to the other considered biological media followed by skin, fat, cornea, liver and bone, respectively. An increase in the effective thermal conductivity results in an increase in the electromagnetic wave penetration causing an increase in the temperature. Also, the maximum temperature difference between the two phases exists in the brain followed by skin, fat, cornea, liver and bone, respectively due to the highest internal heat exchange. However, as can be seen other factors also affect the tissue and blood temperatures such as thermal and dielectric properties and porosity. For example, in case of fat, although it has a low tissue effective thermal conductivity, it also has the lowest porosity and blood effective thermal conductivity resulting in a high temperature.

Figs. 8 and 9 illustrate the effect of variations in the electromagnetic wave power. The dimensionless electromagnetic wave power

of 10, 100 and 500 at $f^* = 0.6$ is considered. Fig. 6 demonstrates the effects of variations in the electromagnetic wave power on the dimensionless temperature contours in the two-dimensional plane of skin. The dimensionless tissue temperature contours are shown in Fig. 8(a), (c) and (e) while Fig. 8(b), (d) and (f) display the dimensionless blood temperature contours. The results clearly show that the tissue and blood temperature values increase with an increase in the electromagnetic wave power. Moreover, an increase in the electromagnetic wave power provides a larger temperature difference between tissue and blood phases as also seen in Fig. 7(a). As can be seen in Fig. 8, the hot spots occur downstream (right-hand side) of the skin slab. The effects of variations in the electromagnetic wave power on the dimensionless temperature contours in the x-y plane of brain are shown in Fig. 9. The dimensionless tissue temperature contours are illustrated in Fig. 9(a), (c) and (e) while Fig. 9(b), (d) and (f) demonstrate the dimensionless blood temperature contours. As can be clearly seen in Fig. 9, once again in an increase in the electromagnetic wave power results in an increase in the tissue and blood temperature values in the brain. Furthermore, an increase in the electromagnetic wave power creates a larger temperature difference between the two phases. These results are consistent with those shown in Fig. 7(b). Similar to the results for the skin the hot spots occur downstream (right-hand side) of the brain slab. It should be noted that for the same impose power, higher temperatures occur within the brain as compared to the skin slab.

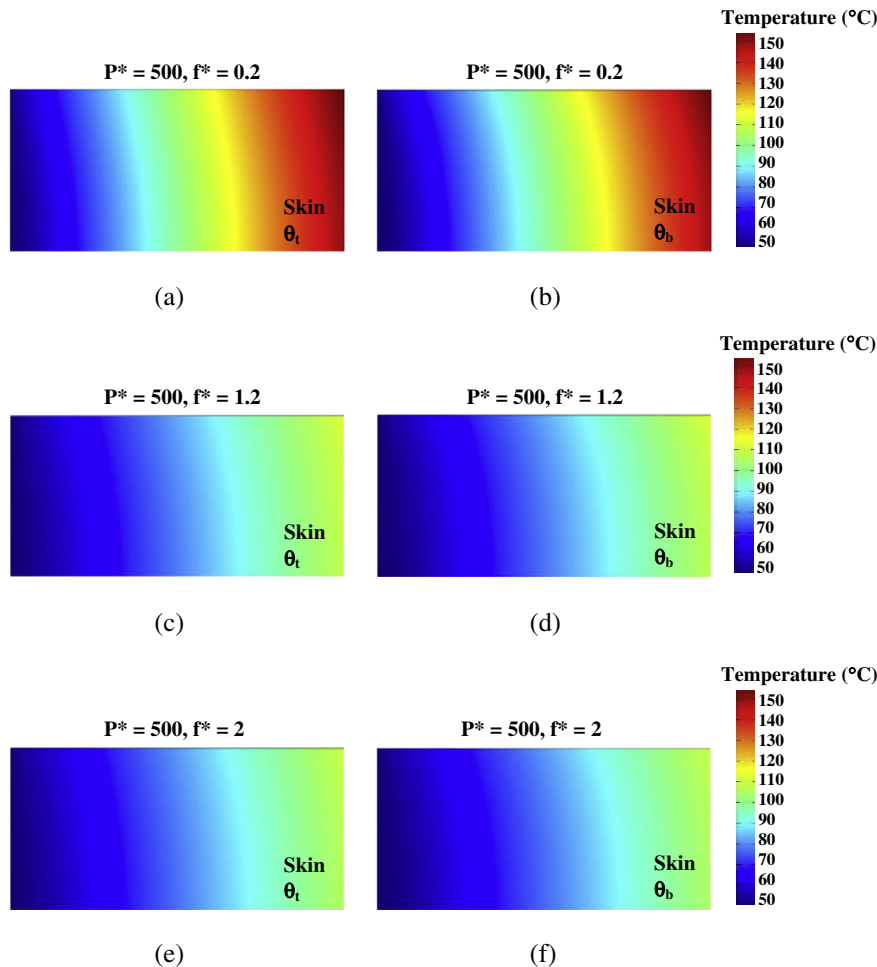


Fig. 13. Tissue and blood temperature contours for skin for $\Phi = 0.1, P^* = 500, Bi = 10$ at various electromagnetic wave frequencies.

5.3. Dimensionless electromagnetic wave frequency effects

Figs. 10–12 shows the effect of variations in the dimensionless electromagnetic wave frequency on the dimensionless tissue and blood temperature profiles for different biological media exposed to an electromagnetic field. The results are shown for: $\Phi = 0.1$ and $P^* = 500$ at $Bi = 10$. The dimensionless electromagnetic wave frequency is varied from 0.2 to 2. The dimensionless tissue and blood temperature profiles for bone, liver, cornea, fat, skin and brain are depicted in Figs. 10(a) and (b), 11(c) and (d) and 12(e) and (f), respectively. The results in these figures show that the temperature profile trend and characteristics are quite similar for all the considered biological media. Note that the highest temperature values do not correspond to the highest electromagnetic wave frequencies. As it can be seen a higher electromagnetic wave frequency produces a lower dimensionless tissue and blood temperature values in all materials. This is because at higher frequencies electromagnetic wave has a shorter wavelength and a smaller penetration depth as compared to lower frequencies. Thus most of electromagnetic energy is absorbed at the entrance region of the biological media. Also it can be seen that the dimensionless blood temperature values are higher than the tissue temperature values for all of the considered biological media subjected to the same electromagnetic wave frequency. Likewise, a decrease in the electromagnetic wave frequency results in a larger deviation between the tissue temperature and that of the blood. This shows that the error in utilizing a LTE model for heat transfer

investigations increases as the wave frequency decreases when an electromagnetic field is imposed. Therefore, the LTNE model needs to be utilized for investigating transport through biological media.

Figs. 13 and 14 demonstrate the effect of variations in the electromagnetic wave frequency. The dimensionless temperature contour plots (Figs. 13 and 14) qualitatively confirm the dimensionless temperature profiles in Fig. 12. The dimensionless electromagnetic wave frequency varies at 0.2, 1.2 and 2 at $P^* = 500$. The influence of dimensionless electromagnetic wave frequency on the temperature contours for the skin at different frequencies are displayed in Fig. 13. The dimensionless tissue temperature contours are shown in Fig. 13(a), (c) and (e) while Fig. 13(b), (d) and (f) depict the dimensionless blood temperature contours. The results show that the tissue and blood temperature values decrease with an increase in the electromagnetic wave frequency. Additionally, a decrease in the electromagnetic wave frequency creates a larger temperature difference between tissue and blood phases which further confirms the results shown in Fig. 12(a). Once again as can be seen in Fig. 13, the hot spots occur on the downstream (right-hand) side of the skin. Fig. 14 shows the effects of variations in the electromagnetic wave frequency on the dimensionless temperature contours of the brain. The dimensionless tissue temperature contours are demonstrated in Fig. 14(a), (c) and (e) whereas Fig. 14(b), (d) and (f) display the dimensionless blood temperature contours. The pattern of temperature contours of the brain are somewhat similar to that of the skin shown in Fig. 13. Again it

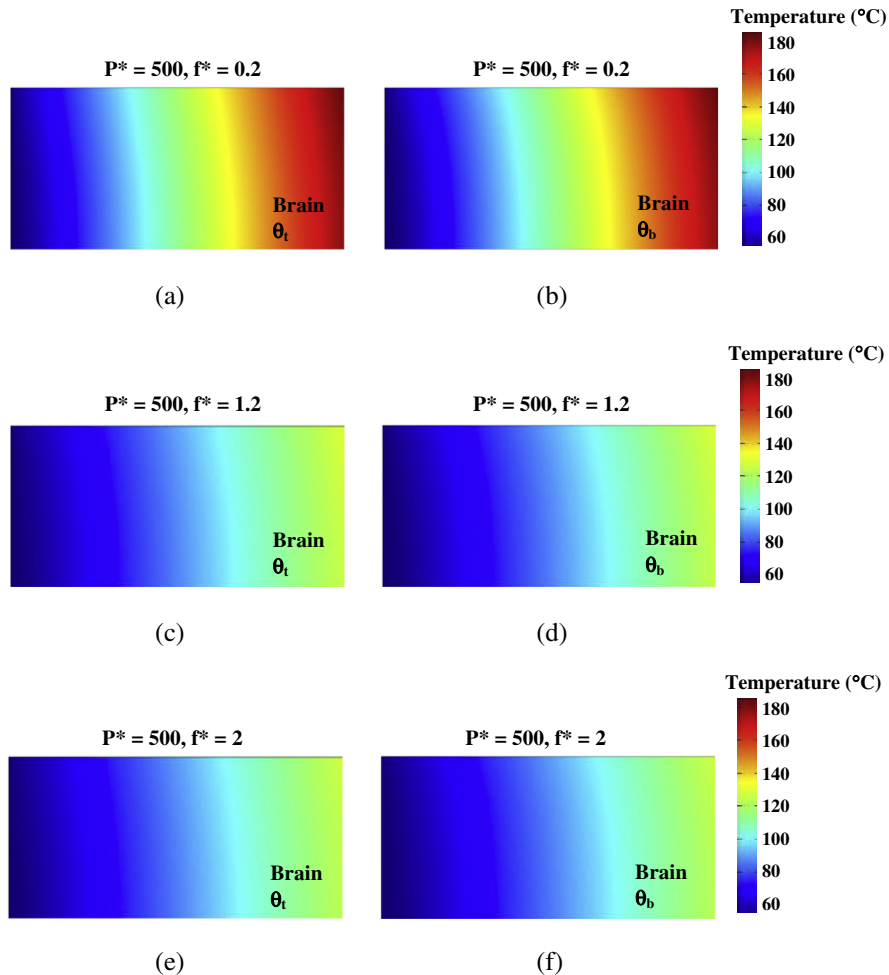


Fig. 14. Tissue and blood temperature contours for brain for $\Phi = 0.1$, $P^* = 500$, $Bi = 10$ at various electromagnetic wave frequencies.

can be observed that a decrease in the electromagnetic wave frequency results in an increase in the tissue and blood temperature values in the brain. In addition, a decrease in the electromagnetic wave frequency results in a larger temperature difference between the two phases. The results in this figure further confirm the results shown in Fig. 12(b). Similar to the situation for the skin, the hot spots occur downstream (right-hand) of the brain slab. It should be noted that the temperature values for the brain are higher than those for the skin at all electromagnetic wave frequencies.

6. Conclusions

In this work, the effects of an imposed electromagnetic field on different biological media is analyzed. The LTNE model is employed to express the heat transport phenomena in a biological medium. The effect of electromagnetic wave power and frequency on heat transport through a biological medium are analyzed. The simulation results are in excellent agreement with the analytical results obtained by Mahjoob and Vafai [8]. The results provide the fundamental attributes of the transport phenomena in biological media subject to an imposed electromagnetic field. The results demonstrate the importance of utilizing the LTNE model especially at lower internal heat exchange values ($Bi = 0.5$), lower porosities and higher metabolic heat generation rates for biological media. The magnitude of electromagnetic wave power and frequency has a substantial impact on the temperature of a biological medium. An increase in the electromagnetic wave power produces a higher tissue and blood temperature and enhances a larger temperature difference between tissue and blood phases. On the other hand, a decrease in the electromagnetic wave frequency produces a higher tissue and blood temperature and results in a larger deviation between the tissue temperature and that of the blood. Our results show that an imposed electromagnetic field has a substantial effect in altering the LTE between tissue and blood phases in biological materials.

Acknowledgments

The authors gratefully acknowledge the financial support for this work provided by the Thailand Research Fund (TRF) and Thammasat University and the Higher Education Research Promotion and National Research University Project of Thailand, Office of the Higher Education Commission.

References

- [1] S. Chatterjee, T. Basak, S.K. Das, Microwave driven convection in a rotating cylindrical cavity: a numerical study, *J. Food Eng.* 79 (2007) 1269–1279.
- [2] G. Carrafiello, D. Laganà, M. Mangini, F. Fontana, G. Dionigi, L. Boni, F. Rovera, S. Cuffari, C. Fugazzola, Microwave tumors ablation: principles, clinical applications and review of preliminary experiences, *Int. J. Surgery* 6 (2008) S65–S69.
- [3] C. Jones, S.A. Badger, G. Ellis, The role of microwave ablation in the management of hepatic colorectal metastases, *The Surgeon* 9 (2011) 33–37.
- [4] G.J. Beers, Biological effects of weak electromagnetic fields from 0 Hz to 200 MHz: a survey of the literature with special emphasis on possible magnetic resonance effects, *Mag. Res. Imaging* 7 (1989) 309–331.
- [5] I.A. Cotgreave, Biological stress responses to radio frequency electromagnetic radiation: are mobile phones really so (heat) shocking?, *Arch Biochem. Biophys.* 435 (2005) 227–240.
- [6] T. Wessapan, S. Srisawatdhisukul, P. Rattanadecho, Numerical analysis of specific absorption rate and heat transfer in the human body exposed to leakage microwave power at 915 MHz and 2450 MHz, *ASME J. Heat Transfer* 133 (2011) 051101-1–051101-13.
- [7] A.-R.A. Khaled, K. Vafai, The role of porous media in modeling flow and heat transfer in biological tissues, *Int. J. Heat Mass Transfer* 46 (2003) 4989–5003.
- [8] S. Mahjoob, K. Vafai, Analytical characterization of heat transport through biological media incorporating hyperthermia treatment, *Int. J. Heat Mass Transfer* 52 (2009) 1608–1618.
- [9] S. Mahjoob, K. Vafai, Analysis of bioheat transport through a dual layer biological media, *ASME J. Heat Transfer* 132 (2010) 031101-1–031101-14.
- [10] P. Keangin, P. Rattanadecho, T. Wessapan, An analysis of heat transfer in liver tissue during microwave ablation using single and double slot antenna, *Int. Commun. Heat Mass Transfer* 38 (2011) 757–766.
- [11] D.Y. Lee, K. Vafai, Analytical characterization and conceptual assessment of solid and fluid temperature differentials in porous media, *Int. J. Heat Mass Transfer* 42 (1999) 423–435.
- [12] B. Alazmi, K. Vafai, Analysis of variants within the porous media transport models, *ASME J. Heat Transfer* 122 (2000) 303–326.
- [13] A. Marafie, K. Vafai, Analysis of non-Darcian effects on temperature differentials in porous media, *Int. J. Heat Mass Transfer* 44 (2001) 4401–4411.
- [14] A. Amiri, K. Vafai, Analysis of dispersion effects and non-thermal equilibrium non-Darcian, variable porosity incompressible flow through porous medium, *Int. J. Heat Mass Transfer* 37 (1994) 939–954.
- [15] A. Amiri, K. Vafai, Transient analysis of incompressible flow through a packed bed, *Int. J. Heat Mass Transfer* 41 (1998) 4259–4279.
- [16] S. Mahjoob, K. Vafai, Analytical characterization and production of an isothermal surface for biological and electronic applications, *ASME J. Heat Transfer* 131 (2009) 052604-1–052604-12.
- [17] S. Mahjoob, K. Vafai, Analysis of heat transfer in consecutive variable cross-sectional domains-applications in biological media and thermal management, *ASME J. Heat Transfer* 133 (2011) 011006-1–011006-9.
- [18] A. Belmiloudi, Parameter identification problems and analysis of the impact of porous media in biofluid heat transfer in biological tissues during thermal therapy, *Nonlinear Anal. Real World Appl.* 11 (2010) 1345–1363.
- [19] N. Afrin, Y. Zhang, J.K. Chen, Thermal lagging in living biological tissue based on nonequilibrium heat transfer between tissue, arterial and venous bloods, *Int. J. Heat Mass Transfer* 54 (2011) 2419–2426.
- [20] A. Nakayama, F. Kuwahara, A general bioheat transfer model based on the theory of porous media, *Int. J. Heat Mass Transfer* 51 (2008) 3190–3199.
- [21] W. Klinbun, K. Vafai, P. Rattanadecho, Electromagnetic field effects on transport through porous media, *Int. J. Heat Mass Transfer* 55 (2012) 325–335.
- [22] K. Yang, K. Vafai, Analysis of temperature gradient bifurcation in porous media—an exact solution, *Int. J. Heat Mass Transfer* 53 (2010) 4316–4325.
- [23] K. Yang, K. Vafai, Analysis of heat flux bifurcation inside porous media incorporating inertial and dispersion effects—an exact solution, *Int. J. Heat Mass Transfer* 54 (2011) 5286–5297.
- [24] P. Rattanadecho, P. Keangin, Numerical study of heat transfer and blood flow in two-layered porous liver tissue during microwave ablation process using single and double slot antenna, *Int. J. Heat Mass Transfer* 58 (2013) 457–470.
- [25] M. Rüegg, B. Blanc, The fat globule size distribution in human milk, *BBA – Lipids Lipid Metab.* 666 (1981) 7–14.
- [26] M.A. Bauman, G.T. Gillies, R. Raghavan, M.L. Brady, C. Pedain, Physical characterization of neurocatheter performance in a brain phantom gelatin with nanoscale porosity: steady-state and oscillatory flows, *Nanotechnology* 15 (2004) 92–97.
- [27] Y. He, H. Liu, R. Himeno, J. Sunaga, N. Kakusho, H. Yokota, Finite element analysis of blood flow and heat transfer in an image-based human finger, *Comput. Biol. Med.* 38 (2008) 555–562.
- [28] R.P. Gilbert, Y. Liu, J.-P. Groby, E. Ogam, A. Wirgin, Y. Xu, Computing porosity of cancellous bone using ultrasonic waves. II: The muscle, cortical, cancellous bone system, *Math. Comput. Model.* 50 (2009) 421–429.
- [29] T. Wessapan, P. Rattanadecho, Specific absorption rate and temperature increase in human eye subjected to electromagnetic fields at 900 MHz, *ASME J. Heat Transfer* 134 (2012) 91101-1–91101-11.
- [30] T. Wessapan, S. Srisawatdhisukul, P. Rattanadecho, Specific absorption rate and temperature distributions in human head subjected to mobile phone radiation at different frequencies, *Int. J. Heat Mass Transfer* 55 (2012) 347–359.